

# Sphalerite $^{40}\text{Ar}/^{39}\text{Ar}$ progressive crushing and stepwise heating techniques

Hua-Ning Qiu\*, Ying-De Jiang

*Key Laboratory of Isotope Geochronology and Geochemistry, Guangzhou Institute of Geochemistry,  
Chinese Academy of Sciences, P.O. Box 1131, 510640 Guangzhou, China*

Received 8 February 2006; received in revised form 14 January 2007; accepted 25 January 2007

Available online 2 February 2007

Editor: C.P. Jaupart

## Abstract

It is difficult to determine the mineralization ages of sulfide deposits because no suitable minerals can be selected for the traditional isotopic dating methods. The  $^{40}\text{Ar}/^{39}\text{Ar}$  method rarely applies well to sulfide minerals because of their trace potassium content and strong radioactivity after irradiation. This preliminary study investigates the possibility of dating the hydrothermal sphalerites by  $^{40}\text{Ar}/^{39}\text{Ar}$  using crushing and heating techniques. The  $^{40}\text{Ar}/^{39}\text{Ar}$  crushing experiments of two sphalerite samples from the Fankou Lead–Zinc Deposit yield well-defined and concordant isochron ages of  $265.8 \pm 1.0$  ( $1\sigma$ ) Ma and  $269.7 \pm 6.2$  Ma corresponding to initial  $^{40}\text{Ar}/^{36}\text{Ar}$  ratios of  $290.7 \pm 2.4$  and  $294.6 \pm 8.1$  respectively. The crushed powders of the later sphalerite yields, with stepwise heating, a flat age spectrum with  $^{40}\text{Ar}/^{39}\text{Ar}$  plateau age of  $267.2 \pm 2.5$  Ma, which define a good isochron with an age of  $271.3 \pm 5.4$  Ma and initial  $^{40}\text{Ar}/^{36}\text{Ar}$  ratio of  $294.0 \pm 1.7$ . This is the first report to distinguish secondary and primary fluid inclusions within sphalerite, to obtain their ages using the crushing technique, and to obtain good concordant ages both of fluid inclusions by crushing and heating of K-containing minerals. We expect progressive crushing and stepwise heating techniques will become an effective approach to  $^{40}\text{Ar}/^{39}\text{Ar}$  dating of the mineralization ages of hydrothermal sulfide deposits.

© 2007 Elsevier B.V. All rights reserved.

**Keywords:**  $^{40}\text{Ar}/^{39}\text{Ar}$  method; fluid inclusion; crushing in vacuum; mineralization age; Fankou Pb–Zn deposit

## 1. Introduction

$^{40}\text{Ar}/^{39}\text{Ar}$  dating is rarely used on sulfide minerals because of their trace potassium content and strong radioactivity after irradiation. The possibility of dating ‘pyrite’ by  $^{40}\text{Ar}/^{39}\text{Ar}$  laser probe has been well-investigated [1–6]. Since Kelley et al. [7] attempted to analyze fluid inclusions by the  $^{40}\text{Ar}/^{39}\text{Ar}$  method using a crushing and gas-extraction technique, it has been demonstrated that fluid inclusions in quartz from

hydrothermal deposits can be dated by crushing in a vacuum [8–14]. Qiu and Wijbrans [15] improved the crusher by creating a spherical curvature on the inside base and developing a  $^{40}\text{Ar}/^{39}\text{Ar}$  crushing technique for 20–50 mg samples and succeeded in dating garnets from the ultra-high-pressure metamorphism eclogites in Dabieshan, central eastern China. A new  $^{40}\text{Ar}/^{39}\text{Ar}$  laboratory with a high sensitivity 5400Ar mass spectrometer from GV Instruments<sup>®</sup> has been established in our institute so that we can investigate the possibility to safely date sulfide samples of ~50 mg by  $^{40}\text{Ar}/^{39}\text{Ar}$  stepwise crushing and heating techniques. To date sulfides directly, rather than the associated K-bearing

\* Corresponding author. Tel.: +86 20 33656389; fax: +86 20 85291510.  
E-mail address: [qiuhn@gig.ac.cn](mailto:qiuhn@gig.ac.cn) (H.-N. Qiu).

hydrothermal phases, is very important for obtaining accurate mineralization ages of the sulfide ore deposits.

### 1.1. Successful applications of $^{40}\text{Ar}/^{39}\text{Ar}$ crushing technique

Three examples in the following show that the  $^{40}\text{Ar}/^{39}\text{Ar}$  crushing technique works to date the fluid inclusions within K-poor minerals.

#### 1.1.1. Coexisting muscovite and quartz from a hydrothermal deposit

Coexisting muscovite S-90MS and quartz S-90Qw were separated from a piece of tungsten ore of the Lushui Tin–tungsten Deposit [10]. The age spectrum of the muscovite S-90MS by stepped heating is essentially flat with a plateau age  $38.8 \pm 0.6$  Ma and isochron age of  $38.6 \pm 0.8$  Ma. Crushing the quartz S-90Qw *in vacuo* yields a smoothly falling age spectrum marked by high ages at low value of  $^{39}\text{Ar}$  release; and its minimum age is higher than that gained from its coexisting muscovite S-90MS, which indicates that some excess  $^{40}\text{Ar}$  was trapped in the fluid inclusions during crystallization. The isochron plot of  $^{40}\text{Ar}/^{36}\text{Ar}$  against  $^{39}\text{Ar}/^{36}\text{Ar}$ , based on argon isotopes released by crushing sample S-90Qw, shows significant chronological information. The line corresponds to an age of  $38.6 \pm 1.9$  Ma, which coincides excellently with the results gained from the stepped heating of coexisting muscovite S-90MS, and agrees within experiment errors with the plateau age of the quartz by stepped heating. Please refer to Qiu et al. (1996) [10] for more details.

#### 1.1.2. Coexisting paragonite and amphibole from a metamorphic vein

A 2.5 m long 0.5–20 cm wide paragonite–amphibole–quartz vein cuts the Zhujiachong cold eclogite in the southern Dabieshan, central eastern China [16]. Coexisting paragonite DB-38MS and amphibole DB-38Amp from the metamorphic vein were analyzed by  $^{40}\text{Ar}/^{39}\text{Ar}$  laser stepwise heating and stepwise crushing respectively. The paragonite subjected to stepwise heating yields a flat age spectrum with a plateau age of  $204 \pm 5$  Ma. The amphibole that underwent stepwise crushing yields a staircase pattern age spectrum in the first twelve steps decreasing to a plateau segment from steps 13 to 25, with an age of  $201 \pm 3$  Ma ( $^{39}\text{Ar}$ : 36.7%). The data points of plateau define a line with isochron age of  $203 \pm 19$  Ma. See Qiu and Wijbrans (2006) [16] for further details.

#### 1.1.3. Coexisting biotite and garnet from a gneiss

Coexisting biotite 02SH03Bi and garnet 02SH03G were selected from a hand-specimen of garnet-bearing

gneiss in Shuanghe, Dabieshan (Qiu and Wijbrans, unpublished data). Laser stepwise heating of the biotite 02SH03Bi forms a flat age spectrum on the whole, with total age of  $455 \pm 2$  Ma, which in detail could be divided into three parts: (1) steps 7–14, corresponding to a plateau age of  $451 \pm 2$  Ma with 48.4% of the total  $^{39}\text{Ar}$  release; (2) steps 15–16, a weighted-mean age of  $460 \pm 2$  Ma with 28.4%  $^{39}\text{Ar}$  release; (3) steps 17–18, a weighted-mean age of  $469 \pm 2$  Ma with 13.5%  $^{39}\text{Ar}$  release. On the normal isochron diagram the data points of steps 7–14 of biotite 02SH03Bi give a well-defined isochron line corresponding to an age of  $455 \pm 4$  Ma. The other data points cluster along the isochron line. All the data points define an isochron age of  $459 \pm 14$  Ma.

The  $^{40}\text{Ar}/^{39}\text{Ar}$  dating results of garnet 02SH03G by stepwise crushing form a similar age spectrum to those garnets of the Bixiling eclogites [15], beginning with an unreasonably high apparent age at first step, decreasing dramatically in the first 10 steps, then decreasing gradually to form a plateau age of  $458 \pm 12$  Ma (23% of  $^{39}\text{Ar}$  release) between steps 18 to 29. Two distinct reservoirs can be inferred from the inverse isochron diagram of  $^{36}\text{Ar}/^{40}\text{Ar}$  vs.  $^{39}\text{Ar}/^{40}\text{Ar}$ : (1) the excess argon reservoir that defines a cloud of points with a positive slope, followed by (2) a well-defined isochron that is based on the data points of steps 18 to 29 corresponding to a negative slope indicating an isochron age of  $451 \pm 53$  Ma, an initial  $^{40}\text{Ar}/^{36}\text{Ar}$  ratio of  $298 \pm 18$ .

All the above isochron ages of K-poor quartz, amphibole and garnet obtained by the  $^{40}\text{Ar}/^{39}\text{Ar}$  crushing technique are well-defined and concordant with those obtained by stepwise heating respectively of their coexisting muscovite, paragonite and biotite. These facts indicate that the  $^{40}\text{Ar}/^{39}\text{Ar}$  crushing technique is an effective approach to date the fluid inclusions within K-poor minerals.

In this preliminary study of the  $^{40}\text{Ar}/^{39}\text{Ar}$  crushing technique applied on sulfides, we report reasonably well-defined age results of two sphalerite samples from the Fankou super-large Lead–Zinc Deposit, Guangdong Province, southern China.

## 2. Geological setting

The Fankou super-large Lead–Zinc Deposit occurs in middle-upper Devonian and lower Carboniferous carbonate and argillaceous carbonate formations [17] in the northern Guangdong Province of southern China. Its mineralization ages have been poorly constrained because the main ore minerals (sphalerite, galena, pyrite and siderite) and the main gangue minerals (calcite and dolomite) are not suitable for the traditional isotopic

dating methods, i.e. K–Ar ( $^{40}\text{Ar}/^{39}\text{Ar}$ ), Rb–Sr, Sm–Nd and U–Pb. Until now, only a few questionable model dates of single-stage lead in galena have been reported [18]: 178 Ma (2 samples), 290 Ma (5 samples) and 398 Ma (1 sample).

There are abundant fluid inclusions within the sphalerites used in this study. The primary fluid inclusions of sphalerite 04FK-11Sp are mainly tubular (5–15  $\mu\text{m}$  in length) and subordinately elliptic (0.5–4  $\mu\text{m}$ ) in shape (Fig. 1a); and those of 04FK-02Sp are mainly elliptic, round (<3  $\mu\text{m}$ ) and subordinately xenomorphic (<5  $\mu\text{m}$ ) in shape (Fig. 1b). Three types of fluid inclusions can be identified [18]: (1) a liquid type (5–20% gases); (2) a gas type (60% gases) and (3) a few inclusions of a one-phase liquid type. It is easy to observe bubbles moving inside some big fluid inclusions. The homogenization temperatures range from 119 to 189  $^{\circ}\text{C}$  with an average of 171  $^{\circ}\text{C}$  [18]. The secondary fluid inclusions are distributed along the microcracks.

### 3. Experimental methods

Hand specimens were crushed in a stainless steel mortar. Single sphalerite minerals of 30–60 meshes in size were separated by hand picking under a binocular

microscope and then cleaned in an ultrasonic bath with deionized water for 15 min.

Samples and a monitor standard DRA1 sanidine [19] with age of  $25.26 \pm 0.07$  Ma were irradiated in the 49–2 reactor in Beijing for 54 h. Correction factors for interfering argon isotopes derived from Ca and K are:  $(^{39}\text{Ar}/^{37}\text{Ar})_{\text{Ca}} = 8.984 \times 10^{-4}$ ,  $(^{36}\text{Ar}/^{37}\text{Ar})_{\text{Ca}} = 2.673 \times 10^{-4}$  and  $(^{40}\text{Ar}/^{39}\text{Ar})_{\text{K}} = 5.97 \times 10^{-3}$ . A sensitivity calibration using an HD-B1 biotite standard ( $3.364 \times 10^{-10}$  mol/g radiogenic  $^{40}\text{Ar}$  content) [20,21] yielded an average value of  $1.64 \times 10^{-15}$  mol  $^{40}\text{Ar}$  per millivolt for our GV5400 mass spectrometer.

In order to obtain  $J$ -values for the samples, the monitor DRA1 was packed between every four samples in quartz tubes, each tube containing 4 packets of DRA1. Based on the  $J$ -values and the positions of DRA1 in the sample tube, a regression line was obtained for each sample tube, and then the  $J$ -values of the samples were calculated by interpolation from the regression line. The  $J$ -value uncertainty of 0.15% ( $1\sigma$ ) was propagated into the age calculations.

The crushing experiments were carried out in an in-house designed crushing apparatus which was connected to the extraction line. The crusher is made of a new type of high-temperature (up to 1200  $^{\circ}\text{C}$ ) stainless steel tube of 210 mm in length and 28 mm in bore diameter. The tube has a spherical curvature on the inside base. The curvature on the dead-weight pestle is of slightly smaller radius than that of the crusher base, allowing concentration of powder to form near the tube central axis during crushing. Samples were crushed by repeatedly lifting and dropping the pestle using an external electromagnet respectively. Prior to analysis, blanks were reduced by heating the whole apparatus to 150  $^{\circ}\text{C}$  using heating tape, and the sample tube was heated to 170  $^{\circ}\text{C}$  using a furnace for *ca.* 10 h. The samples were crushed by repeatedly lifting and dropping the pestle using an external electric magnet with a frequency of 2.5 Hz controlled by an adjustable repeating-timer-relay. The pestle was dropped from a height of 3–5 cm. The pestle drop number of each step is recorded on a digital counter. As it was found that the gas yield decreased during the experiment, the number of the pestle movements for each successive extraction step was increased to maintain the argon concentration levels high enough for measurement.

In order to correct the system blanks, experiments began and ended with cool blank analyses and cool blank analyses were carried out between every four steps of the sample analyses. We noticed that atmospheric argon was released from the crusher in a crushing test without a sample, but it is difficult to correct its contribution at present.

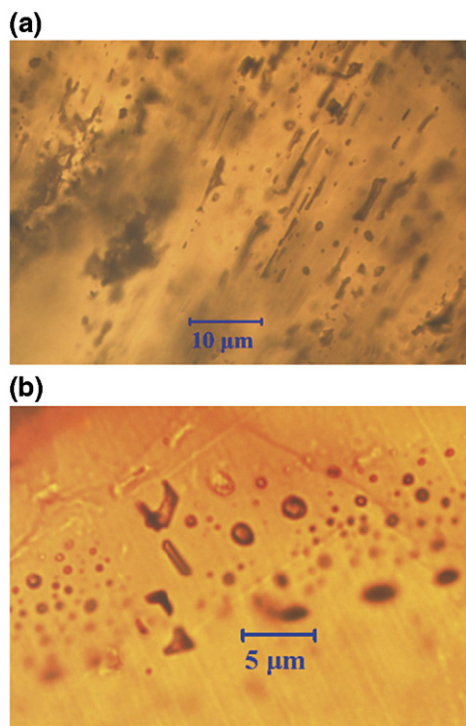


Fig. 1. Photomicrographs of 04FK-11Sp (a) and 04FK-02Sp (b) showing the fluid inclusions inside the sphalerites.

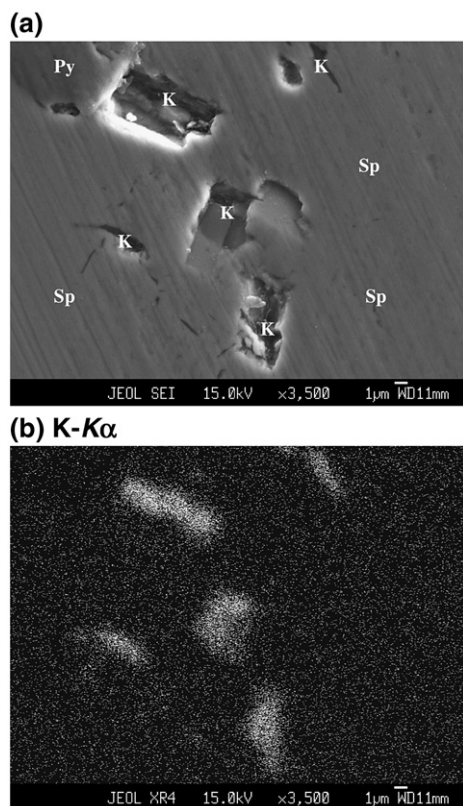


Fig. 2. Images of electron probe microanalyses showing some K-rich microlites inside sphalerite 04FK-02Sp. (a) the secondary electronic image; (b) the K-K $\alpha$  X-ray image. Py: pyrite; Sp: sphalerite; K: potassium-rich microlites.

The crushed powders were heated inside the crusher tube by an external temperature-controlled oven while the pestle was removed from the oven.

The released gases were purified by two Zr/Al getter pumps operated for 5 to 8 min at room temperature and  $\sim 450$  °C respectively. The purified gas was then analyzed for the argon isotopes in a 5400Ar mass spectrometer in our laboratory. The  $^{40}\text{Ar}/^{39}\text{Ar}$  dating results are calculated and plotted using the ArArCALC software by A. A. P. Koppers [22].

In order to interpret the  $^{40}\text{Ar}/^{39}\text{Ar}$  results from the stepwise heating, sphalerite 04FK-02Sp was examined on a new JEOL JXA-8100<sup>®</sup> Electron Probe Micro-analyzer in our institute; and some K-rich silicate microlites (2–10  $\mu\text{m}$ ) were found inside the sphalerite grains (Fig. 2).

#### 4. Results and discussion

Crushing in vacuum is the accepted technique to release gases trapped in fluid inclusions and along cracks and cavities in a crystalline material. Crushing

apparently has very little effect on the gas component that is trapped within the crystal lattice: the crushing experiment on the Methuen muscovite showed that only  $\sim 0.53\%$  of the total  $^{39}\text{Ar}$  was released by crushing [23]. Qiu et al. [12] also indicated that “the gases within the structures of the solid minerals are hardly released by crushing”. Therefore, the results obtained from our sphalerite samples by crushing may be interpreted with some confidence as the contribution of the fluid inclusions trapped inside the crystalline mass. We will discuss this interpretation further in Section 4.2.

##### 4.1. $^{40}\text{Ar}/^{39}\text{Ar}$ dating results

The age spectrum and isochron plots based on the  $^{40}\text{Ar}/^{39}\text{Ar}$  dating results of sphalerites 04FK-11Sp and 04FK-02Sp are shown in Table 1 and in Figs. 3 and 4 respectively. The former was analyzed by progressive crushing, and the latter by progressive crushing and then stepwise heating for the crushed powders within the crusher tube using an external temperature-controlled furnace. The  $^{40}\text{Ar}/^{39}\text{Ar}$  ratios of both the sphalerites as determined from progressive crushing experiments form age spectra with apparent ages decreasing dramatically in the first several steps but finally attaining age plateaux in the last several steps, with plateau ages of  $264.4 \pm 0.7$  Ma ( $1\sigma$ ) (MSWD = 1.78) and  $269.10 \pm 1.0$  Ma (MSWD = 0.79) respectively (Figs. 3a and 4a). On the inverse isochron plots of  $^{36}\text{Ar}/^{40}\text{Ar}$  vs.  $^{39}\text{Ar}/^{40}\text{Ar}$  (see [24] for the interpretation of inverse isochron diagrams), the crushing data points obviously form two groups defining two isochron lines (Figs. 3b and 4b):

(1) The first several steps define isochron lines with concordant ages of  $233.6 \pm 7.4$  Ma (MSWD = 36.9) and  $234.5 \pm 5.7$  Ma (MSWD = 18.7) corresponding to initial  $^{40}\text{Ar}/^{36}\text{Ar}$  ratios of  $702.8 \pm 27.8$  and  $722.4 \pm 26.4$ , much higher than the ratio of the modern atmosphere. Their weighted-mean K/Ca ratios are 0.38 and 0.36 respectively. This group is interpreted as originating from contributions of the secondary fluid inclusions (SFI) bearing excess  $^{40}\text{Ar}$ , because the SFI distributing along the microcracks are easily released by crushing [15].

If the initial  $^{40}\text{Ar}/^{36}\text{Ar}$  ratios are applied to correct the non-radiogenic argon, the ages of the first five steps of 04FK-11Sp are 119.2, 256.4, 231.8, 224.6 and 235.8 Ma with a plateau age of  $232.1 \pm 3.4$  Ma (steps 3–5); and the ages of the first six steps of 04FK-02Sp are 0, 224.0, 239.1, 236.0, 239.0 and 226.6 Ma with a plateau age of  $234.4 \pm 2.7$  Ma (steps 2–6). These plateau ages are in good agreement with the isochron ages. The fact that the concordant plateau ages could be obtained by correcting the non-radiogenic argon with the initial  $^{40}\text{Ar}/^{36}\text{Ar}$  ratios



Table 1  
 $^{40}\text{Ar}/^{39}\text{Ar}$  dating results

Step	Temp (°C)	$^{36}\text{Ar}_{\text{air}}$	$^{37}\text{Ar}_{\text{Ca}}$	$^{38}\text{Ar}_{\text{Cl}}$	$^{39}\text{Ar}_{\text{K}}$	$^{40}\text{Ar}^*$	Age $\pm 1\sigma$ (Ma)	$^{40}\text{Ar}^*$ (%)	$^{39}\text{Ar}_{\text{K}}$ (%)	K/Ca
<i>(a) 04FK-11Sp by crushing, 56 mg, <math>J=0.01123</math></i>										
1	30	1.253	9.425	0.205	4.146	535.64	1617 $\pm$ 6.5	59.1	1.89	0.189
2	80	0.354	16.649	0.070	12.141	309.33	453.9 $\pm$ 1.4	74.7	5.54	0.314
3	100	0.471	35.989	0.076	26.360	513.61	357.0 $\pm$ 1.0	78.7	12.04	0.315
4	150	0.246	27.795	0.032	18.973	324.10	316.6 $\pm$ 0.9	81.7	8.66	0.294
5	200	0.176	38.666	0.025	23.713	366.63	288.8 $\pm$ 0.7	87.5	10.83	0.264
6	300	0.362	60.732	0.012	25.912	373.52	270.7 $\pm$ 0.9	77.7	11.83	0.183
7	400	0.188	84.552	0.006	27.030	381.90	265.7 $\pm$ 0.8	87.3	12.34	0.137
8	500	0.236	96.907	0.006	21.942	310.09	265.7 $\pm$ 0.9	81.6	10.02	0.097
9	540	0.195	95.479	0.006	16.851	236.31	263.8 $\pm$ 1.0	80.4	7.69	0.076
10	240	0.147	38.007	0.001	5.825	80.92	261.5 $\pm$ 1.6	65.0	2.66	0.066
11	240	0.128	33.579	0.002	5.149	71.61	261.8 $\pm$ 1.5	65.4	2.35	0.066
12	240	0.167	30.739	0.001	4.450	62.83	265.5 $\pm$ 2.3	56.0	2.03	0.062
13	240	0.176	40.169	0.001	5.385	74.62	260.9 $\pm$ 1.9	58.9	2.46	0.058
14	240	0.158	37.086	0.004	4.537	63.93	265.0 $\pm$ 2.0	57.8	2.07	0.053
15	360	0.171	50.951	0.004	5.780	80.26	261.4 $\pm$ 2.0	61.3	2.64	0.049
16	420	0.194	50.655	0.006	5.621	79.21	265.0 $\pm$ 2.0	58.0	2.57	0.048
17	450	0.201	47.008	0.006	5.216	73.25	264.2 $\pm$ 2.3	55.2	2.38	0.048
<i>(b) 04FK-02Sp by crushing, 50 mg, <math>J=0.01114</math></i>										
1	50	1.959	5.075	0.110	3.273	547.00	1897 $\pm$ 10	48.6	4.49	0.361
2	100	0.415	9.973	0.034	6.269	251.43	666.5 $\pm$ 2.6	67.2	8.61	0.352
3	150	0.159	10.508	0.012	7.633	165.04	389.4 $\pm$ 1.2	77.8	10.48	0.407
4	200	0.094	13.302	0.002	8.843	151.20	314.6 $\pm$ 0.8	84.4	12.14	0.372
5	200	0.054	12.974	0.001	7.079	113.22	295.9 $\pm$ 0.8	87.5	9.72	0.306
6	150	0.037	9.473	0.000	4.391	68.76	290.1 $\pm$ 0.8	86.1	6.03	0.260
7	150	0.061	8.872	0.000	3.211	51.17	294.8 $\pm$ 1.2	74.1	4.41	0.203
8	150	0.051	9.710	0.000	3.093	48.24	289.1 $\pm$ 1.2	76.3	4.25	0.178
9	150	0.044	8.841	0.001	2.382	37.55	291.9 $\pm$ 2.2	74.2	3.27	0.151
10	150	0.024	7.035	0.001	1.326	22.20	308.4 $\pm$ 2.3	75.8	1.82	0.106
11	150	0.022	7.601	0.000	1.361	21.72	295.3 $\pm$ 1.6	77.1	1.87	0.100
12	225	0.036	11.720	0.001	1.797	28.21	290.8 $\pm$ 1.6	72.7	2.47	0.086
13	225	0.035	11.833	0.001	1.677	25.84	285.8 $\pm$ 1.8	71.4	2.30	0.079
14	225	0.045	11.793	0.001	1.504	22.94	283.2 $\pm$ 2.1	63.2	2.06	0.071
15	225	0.047	11.838	0.001	1.391	21.12	282.0 $\pm$ 2.3	60.6	1.91	0.066
16	300	0.037	15.135	0.002	1.687	25.39	279.7 $\pm$ 1.6	70.0	2.32	0.062
17	325	0.093	15.971	0.001	1.722	25.77	278.2 $\pm$ 3.0	48.4	2.36	0.060
18	340	0.088	16.662	0.001	1.696	24.63	270.5 $\pm$ 2.9	48.6	2.33	0.057
19	345	0.064	15.143	0.001	1.440	21.20	274.0 $\pm$ 2.8	52.8	1.98	0.053
20	345	0.066	14.795	0.001	1.395	20.18	269.7 $\pm$ 2.9	50.8	1.92	0.053
21	380	0.047	14.401	0.000	1.294	18.86	271.6 $\pm$ 2.5	57.7	1.78	0.050
22	400	0.049	13.596	0.001	1.221	17.60	268.7 $\pm$ 2.7	54.8	1.68	0.050
23	450	0.047	13.499	0.000	1.200	17.19	267.2 $\pm$ 2.6	55.2	1.65	0.050
24	550	0.050	13.935	0.002	1.294	18.56	267.5 $\pm$ 2.8	55.8	1.78	0.052
25	550	0.052	12.864	0.003	1.218	17.31	265.2 $\pm$ 2.8	52.7	1.67	0.053
26	610	0.068	11.622	0.003	1.188	16.99	266.7 $\pm$ 3.1	45.8	1.63	0.057
27	600	0.046	9.473	0.001	1.059	15.21	267.9 $\pm$ 3.7	52.8	1.45	0.063
28	750	0.061	9.565	0.002	1.178	16.93	267.9 $\pm$ 3.7	48.4	1.62	0.069
<i>(c) 04FK-02Sp by heating, 50 mg, <math>J=0.01114</math></i>										
Step	Temp (°C)	$^{36}\text{Ar}_{\text{air}}$	$^{37}\text{Ar}_{\text{Ca}}$	$^{38}\text{Ar}_{\text{Cl}}$	$^{39}\text{Ar}_{\text{K}}$	$^{40}\text{Ar}^*$	Age $\pm 1\sigma$ (Ma)	$^{40}\text{Ar}^*$ (%)	$^{39}\text{Ar}_{\text{K}}$ (%)	K/Ca
1	200	0.026	0.077	0.000	0.052	0.87	311.4 $\pm$ 35.8	10.2	0.44	0.374
2	240	0.079	0.156	0.000	0.161	2.77	315.9 $\pm$ 25.1	10.6	1.39	0.580
3	280	0.100	0.234	0.000	0.340	5.22	285.3 $\pm$ 14.5	15.1	2.93	0.811
4	320	0.094	0.336	0.001	0.531	8.05	281.5 $\pm$ 8.9	22.5	4.58	0.885

Table 1 (continued)

Step	Temp (°C)	$^{36}\text{Ar}_{\text{air}}$	$^{37}\text{Ar}_{\text{Ca}}$	$^{38}\text{Ar}_{\text{Cl}}$	$^{39}\text{Ar}_{\text{K}}$	$^{40}\text{Ar}^*$	Age $\pm 1\sigma$ (Ma)	$^{40}\text{Ar}^*$ (%)	$^{39}\text{Ar}_{\text{K}}$ (%)	K/Ca
5	360	0.114	0.606	0.001	0.898	13.31	275.9 $\pm$ 5.7	28.3	7.73	0.830
6	400	0.119	1.061	0.002	1.185	17.09	268.9 $\pm$ 4.8	32.7	10.20	0.625
7	440	0.129	1.779	0.001	1.210	17.44	268.5 $\pm$ 4.8	31.4	10.42	0.381
8	480	0.120	2.529	0.001	0.976	14.01	267.7 $\pm$ 5.9	28.3	8.41	0.216
9	520	0.201	4.933	0.001	0.898	12.84	266.6 $\pm$ 10.6	17.8	7.74	0.102
10	560	0.195	5.031	0.001	0.804	11.49	266.5 $\pm$ 11.4	16.6	6.93	0.090
11	600	0.250	4.752	0.001	0.884	12.50	263.9 $\pm$ 12.3	14.5	7.61	0.104
12	640	0.267	3.337	0.001	0.864	12.31	265.7 $\pm$ 14.3	13.5	7.44	0.145
13	680	0.230	2.027	0.001	0.696	9.78	262.6 $\pm$ 14.7	12.6	5.99	0.192
14	720	0.240	2.224	0.002	0.751	10.56	262.7 $\pm$ 14.4	13.0	6.47	0.189
15	760	0.215	2.455	0.002	0.699	9.80	261.8 $\pm$ 13.5	13.4	6.02	0.160
16	800	0.203	2.650	0.003	0.662	9.27	261.8 $\pm$ 12.9	13.4	5.70	0.140

The argon isotopes are listed in millivolt. The multiplier sensitivity of this 5400Ar mass spectrometer is  $1.64 \times 10^{-15}$  mol/mV.

indicates that the gases of the first several crushing steps are mainly released from the secondary fluid inclusions. Thus this age of  $\sim 233$  Ma should represent a separate post-mineralization pulse of fluid of quite different composition (see further discussion in Section 4.2).

(2) The last several steps defining the age plateau yield well-defined isochron lines with ages of  $265.8 \pm 1.0$  Ma (MSWD=1.38) and  $269.7 \pm 6.2$  Ma (MSWD=0.88), corresponding to initial  $^{40}\text{Ar}/^{36}\text{Ar}$  ratios of  $290.7 \pm 1.0$  and  $294.6 \pm 8.1$  which are close to the modern atmospheric ratio of 295.5. Their weighted-mean K/Ca ratios are 0.11 and 0.06 respectively, much lower than the ratios of the first several steps (SFI). This group is interpreted as the contributions from the radiogenic and trapped argon in the primary fluid inclusions (PFI) and the trapped modern air in the crusher. Although the crusher atmospheric argon cannot be corrected exactly at present, the isochron age and initial  $^{40}\text{Ar}/^{36}\text{Ar}$  (Figs. 3b and 4b) can represent the true

situations of PFI because the signals of the argon isotopes are sufficiently high in all crushing steps for precise analyses, and the  $^{40}\text{Ar}^*$  concentrations are higher than 48% (Table 1a, b). The initial  $^{40}\text{Ar}/^{36}\text{Ar}$  ratios of  $\sim 295$  indicate no excess  $^{40}\text{Ar}$  within the PFI. The atmosphere argon isotopic composition implies that the trapped argon within the PFI might dissolve the palaeo-atmospheric argon, which supports the conclusions that “isotopic studies indicate that most of the Pb and S are sedimentary origin” and that the Fankou deposit belongs to a strongly reformed post-sedimentary deposits suggested by Tu Kuang-chih (1981) [25].

The crushed powders of 02FK-02Sp were further analyzed by  $^{40}\text{Ar}/^{39}\text{Ar}$  stepwise heating from 200 to 800 °C with temperature increments of 40 °C per step, using an external temperature-controlled oven directly outside the crushing tube, the pestle being drawn out during heating. The results yield a flat age spectrum (the

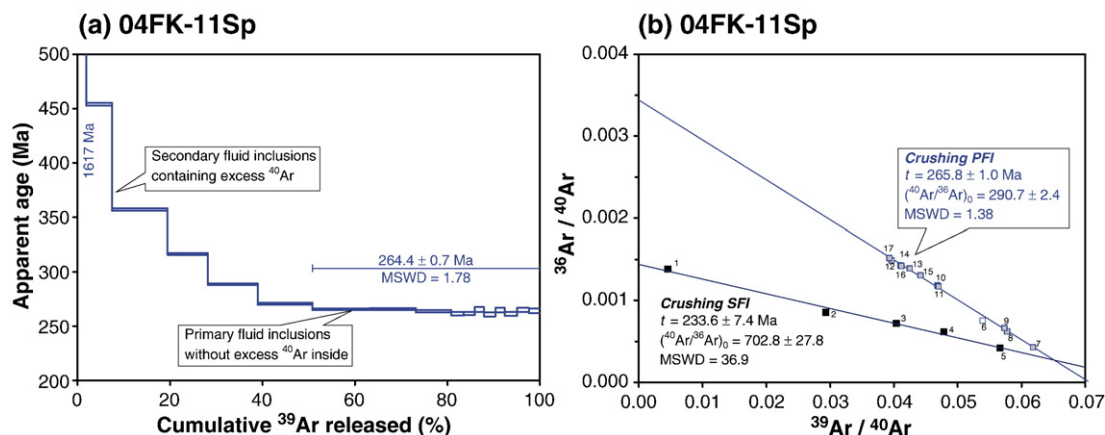


Fig. 3.  $^{40}\text{Ar}/^{39}\text{Ar}$  age spectrum and inverse isochron lines of sphalerite 04FK-11Sp by progressive crushing.

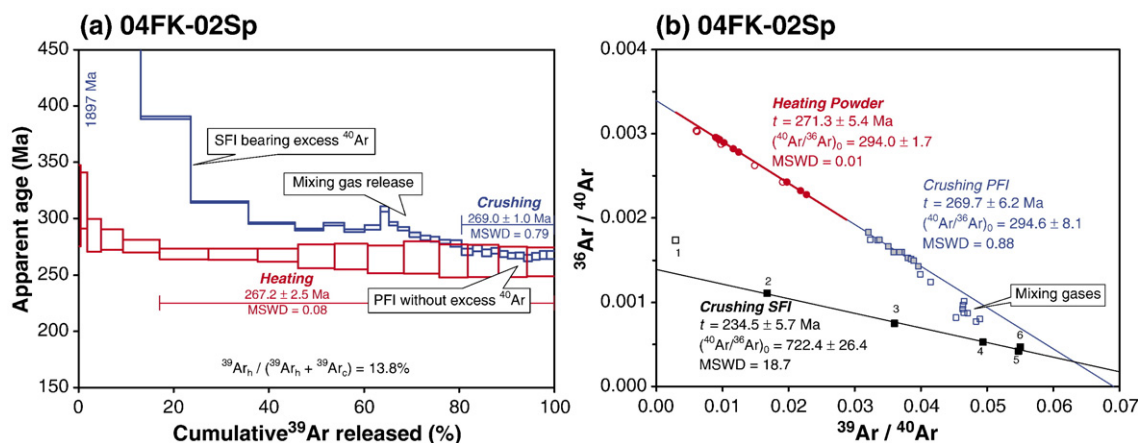


Fig. 4.  $^{40}\text{Ar}/^{39}\text{Ar}$  age spectra and inverse isochron lines of sphalerite 04FK-02Sp by progressive crushing and stepwise heating. (For interpretation of the references to colour in this figure legend, the reader is referred to the web version of this article.)

red lines in Fig. 4a) with a plateau age of  $267.2 \pm 2.5$  Ma (from 400 to 800 °C, 82.9% of  $^{39}\text{Ar}$  released). The data forming the plateau clearly define an isochron with an age of  $271.3 \pm 5.4$  Ma (MSWD=0.01) and an initial  $^{40}\text{Ar}/^{36}\text{Ar}$  ratio of  $294.0 \pm 1.7$  (the red line in Fig. 4b). The weighted-mean K/Ca ratio is 0.24. Obviously, the isochron line from the stepwise heating method is nearly an extension of the PFI line obtained by the crushing method (Fig. 4b) with close agreement of the isochron ages and initial  $^{40}\text{Ar}/^{36}\text{Ar}$  ratios. The gases released during the low temperature steps (<400 °C) may be mixtures from the residual very fine fluid inclusions (<1  $\mu\text{m}$ ) and from the mineral crystal lattices. However, during the further high-temperature steps (400–800 °C), the gas released from the K-rich microlites should be the major contributions to the age spectrum. The isochron derived from the heating method should result from the mixing of the radiogenic argon from K-rich microlites with the modern atmospheric argon from the crusher. In comparison to the crushing experiment, the heating experiment increases the release of atmospheric argon from the crusher, and the  $^{40}\text{Ar}^*$  concentrations are much lower in each step (Table 1). The higher atmospheric argon and lower  $^{40}\text{Ar}^*$  cause larger age errors (Table 1 and Fig. 4a), but the isochron and plateau ages are still quite reliable. This is the first report to obtain good agreement between the ages of fluid inclusions obtained by crushing and from K-rich minerals by heating.

#### 4.2. Gases reservoirs released by crushing and heating

The crushing and heating experiments of sphalerite 04FK-02Sp yield concordant  $^{40}\text{Ar}/^{39}\text{Ar}$  isochron ages and initial  $^{40}\text{Ar}/^{36}\text{Ar}$  ratios, but quite different K/Ca ratios. The K/Ca ratios of 04FK-11Sp (steps 10–17)

and 04FK-02Sp (steps 18–28) by crushing are concordant from 0.05 to 0.07, with averages of 0.056 and 0.055. On the other hand the K/Ca ratios of 04FK-02Sp obtained by heating during steps 9–16 range from 0.1 to 0.2 with an average of 0.14, much higher than those ratios obtained by crushing experiments. The distinct differences of K/Ca ratios indicate that the gases released by crushing and by heating should come from different sources.

Gases from the secondary fluid inclusions distributed along microcracks are easily extracted by crushing. Therefore, in the first five crushing steps, gases with high K/Ca ratios of >0.2 and obvious excess  $^{40}\text{Ar}$  might be released from the secondary fluid inclusions.

Because the ore deposit occurs in middle-upper Devonian and lower Carboniferous carbonate rocks, the ore-forming fluid might have dissolved the carbonate rocks and obtained a high calcium concentration so that the primary fluid inclusions have low K/Ca ratios. Therefore, it makes sense that the gases with low K/Ca ratios of <0.07, released by crushing after the secondary fluid inclusions were extracted in the first several steps, should come from the primary fluid inclusions inside the sphalerites.

The EPMA analyses indicate some K-rich silicate microlites (2–10  $\mu\text{m}$ ) existing inside sphalerite 04FK-02Sp (Fig. 2). Annealing-simulation experiments [26] showed that the sphalerite rims were decomposed and that sulfur released at 550 °C. The stepwise heating experiment of the crushed sphalerite powders 04FK-02Sp (Table 1c) yields higher K/Ca ratios of >0.2 during the 200–480 °C steps and lower K/Ca ratios of <0.2 for the 520–800 °C steps. We speculate that the gases with higher K/Ca ratios at lower temperature steps (<500 °C) are released from the very fine fluid

inclusions (<1  $\mu\text{m}$ ) and possible potassium sub-minerals, while the gases with lower K/Ca ratios at higher temperature steps (>500  $^{\circ}\text{C}$ ) are released from the K-rich silicate microlites.

## 5. Conclusions

This preliminary study obtains good  $^{40}\text{Ar}/^{39}\text{Ar}$  isochron ages of sphalerites by stepwise crushing and heating for the Fankou Pb–Zn Deposit. We intend to investigate more sulfide samples using both the  $^{40}\text{Ar}/^{39}\text{Ar}$  crushing technique and the Rb–Sr method because the potassium concentrations of the sphalerites are higher than in most of the hydrothermal quartz samples analyzed before [10,12]. Some important points emerging from this preliminary study are summarized as follows:

- (1) Progressive crushing and stepwise heating techniques are useful in obtaining precision  $^{40}\text{Ar}/^{39}\text{Ar}$  isochron ages for sphalerite and other sulfide minerals. This suggests an effective approach to dating the mineralization ages of hydrothermal sulfide deposits.
- (2) Primary fluid inclusions may be distinguished from the secondary ones using our progressive crushing technique and in some cases can probably lead to determination of their respective ages.
- (3) The distinct differences among K/Ca ratios indicate that the gases released by crushing and by heating should come from different sources. The gases within the mineral solid phases are hardly released by crushing.
- (4) The well-defined and concordant isochron ages of the PFI obtained using the crushing method, and of the K-rich microlites by stepwise heating, definitely indicate that a mineralization epoch of the Fankou Pb–Zn Deposit took place *ca.* 265–270 Ma ago.
- (5) False isochrons might be obtained if the techniques of  $^{40}\text{Ar}/^{39}\text{Ar}$  stepwise heating or Rb–Sr acid solution [27,28] were directly applied to sphalerite grains because the parent  $^{40}\text{K}$  (or  $^{87}\text{Rb}$ ) and daughter  $^{40}\text{Ar}$  (or  $^{87}\text{Sr}$ ) in the secondary and primary fluid inclusions and in the K-rich microlites would be mixed together.

## Acknowledgements

We would like to thank Dr. Claude P. Jaupart and the anonymous reviewer for their comments that substantially

improved this manuscript. Dr. John Woodside in Vrije Universiteit Amsterdam kindly embellished the English. Mr. Shuiping Xu and Mr. Shenbo Liu helped us during the fieldwork. This work was supported by the National Natural Science Foundation of China (40472048).

## References

- [1] D. York, A. Masliwec, P. Kuybida, J.A. Hanes, C.M. Hall, W.J. Kenyon, E.T.C. Spooner, S.D. Scott,  $^{40}\text{Ar}$ – $^{39}\text{Ar}$  dating of pyrite, *Nature* 300 (1982) 52–53.
- [2] C. Fan, B.Q. Zhu, Z. Pu, Q. Zhang, G. Dai, Investigation on pyrite  $^{39}\text{Ar}$ – $^{40}\text{Ar}$  dating, Third Chinese Conference on Isotope Geochemistry, Yichang, 1986, pp. 249–250.
- [3] P.E. Smith, N.M. Evensen, D. York, P. Szatmari, D.C. de Oliveira, Single-crystal  $^{39}\text{Ar}$ – $^{40}\text{Ar}$  dating of pyrite: no fool's clock, *Geology* 29 (2001) 403–406.
- [4] D. Phillips, J.M. Miller, Testing time for the fool's clock:  $^{40}\text{Ar}/^{39}\text{Ar}$  dating of pyrite, *Geochim. Cosmochim. Acta* 69 (2005) A567.
- [5] P.E. Smith, N.M. Evensen, D. York, S. Moorbath, Oldest reliable terrestrial  $^{40}\text{Ar}$ – $^{39}\text{Ar}$  age from pyrite crystals at Isua west Greenland, *Geophys. Res. Lett.* 32 (2005) L21318.
- [6] D. Phillips, J.M. Miller,  $^{40}\text{Ar}/^{39}\text{Ar}$  dating of mica-bearing pyrite from thermally overprinted Archean gold deposits, *Geology* 34 (2006) 397–400.
- [7] S. Kelley, G. Turner, A.W. Butterfield, T.J. Shepherd, The source and significance of argon isotopes in fluid inclusions from areas of mineralization, *Earth Planet. Sci. Lett.* 79 (1986) 303–318.
- [8] G. Turner, M.P. Bannon, Argon isotope geochemistry of inclusion fluids from granite-associated mineral veins in Southwest and Northeast England, *Geochim. Cosmochim. Acta* 56 (1992) 227–243.
- [9] R. Burgess, S.P. Kelley, I. Parsons, F.D.L. Walker, R.H. Worden,  $^{40}\text{Ar}$ – $^{39}\text{Ar}$  analysis of perthite microtextures and fluid inclusions in alkali feldspars from the Klokken Syenite, South Greenland, *Earth Planet. Sci. Lett.* 109 (1992) 147–167.
- [10] H.N. Qiu,  $^{40}\text{Ar}$ – $^{39}\text{Ar}$  dating of the quartz samples from two mineral deposits in western Yunnan (SW China) by crushing in vacuum, *Chem. Geol.* 127 (1996) 211–222.
- [11] M.A. Kendrick, R. Burgess, R.A.D. Patrick, P.G. Turner, Halogen and Ar–Ar age determinations of inclusions within quartz veins from porphyry copper deposits using complementary noble gas-extraction techniques, *Chem. Geol.* 177 (2001) 351–370.
- [12] H.N. Qiu, B.Q. Zhu, D.Z. Sun, Age significance interpreted from  $^{40}\text{Ar}$ – $^{39}\text{Ar}$  dating of quartz samples from the Dongchuan Copper Deposits, Yunnan, SW China, by crushing and heating, *Geochim. J.* 36 (2002) 475–491.
- [13] G. Turner, Hydrothermal fluids and argon isotopes in quartz veins and cherts, *Geochim. Cosmochim. Acta* 52 (1988) 1443–1448.
- [14] G. Turner, S. Wang, R. Burgess, M. Bannon, Argon and other noble-gases in fluid inclusions, *Chem. Geol.* 70 (1988) 42.
- [15] H.N. Qiu, J.R. Wijbrans, Paleozoic ages and excess  $^{40}\text{Ar}$  in garnets from the Bixiling eclogite in Dabieshan, China: new insights from  $^{40}\text{Ar}/^{39}\text{Ar}$  dating by stepwise crushing, *Geochim. Cosmochim. Acta* 70 (2006) 2354–2370.
- [16] H.N. Qiu, J.R. Wijbrans, Amphibole-lite-facies overprinting and a hydrothermal activity in southern Dabie terrane: insight from Ar–Ar dating of Zhujiachong eclogite and metamorphic Amphibole vein, *Geochimica* 35 (2006) 517–524.



- [17] X.X. Song, Minor elements and ore genesis of the Fankou Lead–Zinc Deposit, China, *Miner. Depos.* 19 (1984) 95–104.
- [18] H.Z. Lu, On the genesis of Fankou Pb–Zn Ore Deposit in Guangdong Province, *Geochimica* 13 (1984) 357–365.
- [19] J.R. Wijbrans, M.S. Pringle, A.A.P. Koppers, R. Scheveers, Argon geochronology of small samples using the vulkaan argon laserprobe, *Proc. K. Ned. Akad. Wet.: Biol., Chem., Geol., Phys., Med. Sci.* 98 (1995) 185–218.
- [20] H.J. Lippolt, J. Hess, Compilation of K–Ar measurements on HD-B1 standard biotite 1994 status report, in: G.S. Odin (Ed.), *Phanerozoic Timescale 12*, IUGS Subcommission on Geochronology, 1994, pp. 18–23.
- [21] U. Fuhrmann, H.J. Lippolt, J.C. Hess, Examination of some proposed K–Ar standards- $^{40}\text{Ar}$ – $^{39}\text{Ar}$  analyses and conventional K–Ar data, *Chem. Geol.* 66 (1987) 41–51.
- [22] A.A.P. Koppers, ArArCALC — software for  $^{40}\text{Ar}/^{39}\text{Ar}$  age calculations, *Comput. Geosci.* 28 (2002) 605–619.
- [23] W.J. Dunlap, A.K. Kronenberg, Argon loss during deformation of micas: constraints from laboratory deformation experiments, *Contrib. Mineral. Petrol.* 141 (2001) 174–185.
- [24] Y.D. Kuiper, The interpretation of inverse isochron diagrams in  $^{40}\text{Ar}/^{39}\text{Ar}$  geochronology, *Earth Planet. Sci. Lett.* 203 (2002) 499–506.
- [25] K.-C. Tu, Genetic classification of Pb–Zn deposits in China, *Annual reports of Institute of Geochemistry, Chinese Academy of Sciences (1978–1979)*, Guizhou People's Publishing House, Guiyang, 1981, pp. 3–4, (in Chinese, with English abstract).
- [26] X.-P. Qiu, C.-J. Wu, Annealing-simulated experiments on lead–zinc ores and wallrocks from Fankou Lead–Zinc Deposits, *Acta Geol. Sin.-Chin.* 20 (1999) 289–293.
- [27] S. Nakai, A.N. Halliday, S.E. Kesler, H.D. Jones, Rb–Sr dating of sphalerites from Tennessee and the genesis of Mississippi Valley type ore deposits, *Nature* 346 (1990) 354–357.
- [28] T. Pettke, L.W. Diamond, Rb–Sr dating of sphalerite based on fluid inclusion-host mineral isochrons: a clarification of why it works, *Econ. Geol. Bull. Soc. Econ. Geol.* 91 (1996) 951–956.